A Combined Hybridized Discontinuous Galerkin / Hybrid Mixed Method For Viscous Conservation Laws

J. Schütz, M. Woopen, G. May

RWTHAACHEN
UNIVERSITY

List of AICES technical reports: http://www.aices.rwth-aachen.de/preprints

A COMBINED HYBRIDIZED DISCONTINUOUS GALERKIN / HYBRID MIXED METHOD FOR VISCOUS CONSERVATION LAWS

Jochen Schütz,

IGPM, RWTH Aachen University
Templergraben 55
52062 Aachen, Germany

Michael Woopen and Georg May

AICES, RWTH Aachen University
Schinkelstraße 2
52062 Aachen, Germany

Abstract. Recently, we have proposed a method for solving steady-state convection-diffusion equations, including the full compressible Navier-Stokes equations [17]. The method is a combination of a mixed Finite Element method for the diffusion terms, and a Discontinuous Galerkin method for the convection term. The method is fully implicit, and the globally coupled unknowns are the hybrid variables, i.e., variables having support on the skeleton of the mesh only. This reduces the amount of overall degrees of freedom tremendously. In this paper, we extend our method to be able to cope with time-dependent convection-diffusion equations, where we use a dual time-stepping method in combination with backward difference schemes.

1. Introduction

Based on recent work on high-order methods, especially Discontinuous Galerkin methods [1, 6, 10], we have proposed a method for solving steady-state convection-diffusion equations in [17], based on the work by Egger and Schöberl [7]. The method combines a mixed Finite Element method for the diffusion terms, and a Discontinuous Galerkin method for the convection terms. It turned out to be actually very similar to a hybridized DG method proposed by Nguyen et al. [14, 15, 16], see also [18] for a comparison of both methods with respect to asymptotic performance.

For stationary and (weakly-)instationary applications in aerodynamics, implicit methods are very popular, as they allow for large time-steps and thus an efficient solution process [12, 13]. Arguably, most popular implicit methods rely on the use of a Newton-type solver, i.e., one needs the Jacobian of the discretization. Typically, for Discontinuous Galerkin methods, the size of this matrix is $O(N \cdot p^{2d})$, where N is the number of elements in the triangulation, p is the underlying degree of polynomial and d is the spatial dimension. Available memory then usually poses a severe restriction on both N and p.

A known way to reduce the size of the Jacobian that has gained some attention recently is the use of hybridization [3, 5]. Roughly speaking, instead of considering

ansatz functions having support in the interior of the elements, one considers ansatz functions whose support is the skeleton of the mesh. For a hybridized Discontinuous Galerkin method, the Jacobian is of size $O(\widehat{N} \cdot p^{2(d-1)})$, where $\widehat{N}$ is the number of edges. Typically, this yields a reduction of the Jacobian size, which implies less storage requirements and, usually, a faster iterative solution process.

In this paper, we extend the method proposed in [17] to cope with time-dependent problems. Time discretization relies on $A(\alpha)$-stable backward difference schemes. We will give the definition of the method and show numerical results.

2. Underlying Equations

Let $\Omega \subset \mathbb{R}^2$ be a domain. For a given system size m, fluxes $f : \mathbb{R}^m \to \mathbb{R}^{m \times 2}$ and $f_v : \mathbb{R}^m \times \mathbb{R}^{m \times 2} \to \mathbb{R}^{m \times 2}$, we consider viscous balance laws, given in mixed form as

$$(1) \qquad \sigma = \nabla w, \quad w_t + \nabla \cdot (f(w) - f_v(w, \sigma)) = g \quad \forall (x, t) \in \Omega \times (0, \infty),$$

equipped with suitable initial and boundary conditions.

A case of particular interest is that of time-dependent Navier-Stokes equations, where the unknowns $w := (\rho, \rho u, \rho v, E)^T$ are density, momentum and total energy, and the fluxes $f \equiv (f^1, f^2)$ and $f_v \equiv (f_v^1, f_v^2)$ are defined as

$$(2) \quad f_1 = (\rho u, p + \rho u^2, \rho uv, u(E + p))^T, \qquad f_2 = (\rho v, \rho uv, p + \rho v^2, v(E + p))^T,$$

$$(3) \quad f_v^1 = (0, \tau_{11}, \tau_{21}, \tau_{11} u + \tau_{12} v + kT_{x_1})^T, \quad f_v^2 = (0, \tau_{12}, \tau_{22}, \tau_{21} u + \tau_{22} v + kT_{x_2})^T.$$

Here p is the pressure, related to the other variables via the ideal gas law. Furthermore, τ denotes the stress tensor, T is the temperature, and k is the thermal conductivity coefficient. For the Navier-Stokes equations, $g \equiv 0$.

Boundary conditions on a surface, e.g., an airfoil, are set as adiabatic, no-slip boundary conditions, i.e., one sets $(u, v) \equiv 0$ and $n \cdot \nabla T \equiv 0$. In- and outflow boundary conditions are set via a characteristic splitting of the convective flux.

3. Method

In the sequel, we will work on a regular triangulation of $\Omega \subset \mathbb{R}^2$. For the necessary notation, we make the following definition:

Definition 3.1 (Triangulation). Let Ω be regularly triangulated as $\Omega = \bigcup_{k=1}^{N} \Omega_k$. We define an edge e_k as an intersection of two neighboring elements, or an element with the physical boundary $\partial \Omega$, having positive one-dimensional measure. Γ denotes the collection of all these intersections, while $\Gamma_0 \subset \Gamma$ denotes those $e_k \in \Gamma$ that do not intersect the physical boundary $\partial \Omega$ of the domain. We define $\widehat{N} := |\Gamma|$ to be the number of edges in Γ.

To simplify the notation, we introduce the following abbreviations for integration:

$$(f_1, f_2) := \sum_{k=1}^{N} \int_{\Omega_k} f_1 \cdot f_2 \, dx,$$

$$\langle f_1, f_2 \rangle_\Gamma := \sum_{k=1}^{\widehat{N}} \int_{e_k} f_1 \cdot f_2 \, d\sigma, \quad \langle f_1, f_2 \rangle_{\partial \Omega_k} := \sum_{k=1}^{N} \int_{\partial \Omega_k} f_1 \cdot f_2 \, d\sigma$$

The method to be presented depends on a triple of function spaces. For a given triangulation, we thus make the following definition:

Definition 3.2. For the approximation of $\sigma_h \approx \nabla w$, $w_h \approx w$ and $\lambda_h \approx w_{|\Gamma}$, we consider the following spaces:

$$V_h := \{f \in L^2(\Omega) | f_{|\Omega_k} \in \Pi^p(\Omega_k) \quad \forall k = 1, \dots N\}^m$$
$$H_h := \{f \in L^2(\Omega) | f_{|\Omega_k} \in \Pi^q(\Omega_k) \quad \forall k = 1, \dots N\}^{2 \cdot m}$$
$$M_h := \{f \in L^2(\Gamma) | f_{|e_k} \in \Pi^q(e_k) \quad \forall k = 1, \dots \widehat{N}\}^m.$$

Recall that m denotes the dimension of the system, i.e., $m = 4$ for the Navier-Stokes equations, and $m = 1$ for a scalar equation. $\Pi^p(U)$ is the space of polynomials up to order p on a domain U. On the relation of p and q, see Remark 1.

Remark 1. For $q = p+1$, our method will be inspired by a Hybrid Mixed method [2], while for $q = p$, it is indeed a hybridized Discontinuous Galerkin method [14, 15, 18]. We will demonstrate numerical results for both choices.

We start by semi-discretizing (1) in a straightforward, DG-like manner as

$$(\sigma_h - \nabla w_h, \tau_h) - \langle \lambda_h - w_h, \tau_h^- \cdot n\rangle_{\partial\Omega_k} = 0 \qquad \forall \tau_h \in H_h$$
$$((w_h)_t, \varphi_h) - (f(w_h) - f_v(w_h, \sigma_h), \nabla\varphi_h) + \langle(\widehat{f} - \widehat{f_v}) \cdot n, \varphi_h^-\rangle_{\partial\Omega_k} = (g, \varphi_h) \quad \forall \varphi_h \in V_h$$
$$\langle[(\widehat{f} - \widehat{f_v})] \cdot n, \mu_h\rangle_\Gamma = 0 \qquad \forall \mu_h \in M_h$$

with numerical fluxes

$$\widehat{f} := f(\lambda_h) - \beta\left(\lambda_h - w_h^-\right) n, \quad \widehat{f_v} := f_v(\lambda_h, \sigma_h^-) + \gamma\left(\lambda_h - w_h^-\right) n.$$

$[\cdot]$ denotes the jump of a quantity; β is Lax-Friedrich's parameter and γ a penalty parameter resulting from a local DG discretization. Note that $\gamma \equiv 0$ for the Hybrid Mixed method. Boundary conditions are incorporated by changing w_h and λ_h on boundary edges accordingly to achieve both a consistent and adjoint consistent scheme. For more details, see [18].

In shorthand notation, the scheme can be written as

$$(4) \qquad T((w_h)_t, \varphi_h) + N(\sigma_h, w_h, \lambda_h; \tau_h, \varphi_h, \mu_h) = 0,$$

where we have suppressed the fact that this has to hold for all $(\tau_h, \varphi_h, \mu_h)$ in the corresponding spaces. T denotes the vector having 0 entries for the first and the last equation, i.e.,

$$T((w_h)_t, \varphi_h) := (0_{\dim(H_h)}, ((w_h)_t, \varphi_h), 0_{\dim(M_h)})^T.$$

Remark 2. Note that the very special form of T is the reason that a straightforward explicit method of lines approach is not possible, because T only involves temporal derivatives of w_h, but not of σ_h and λ_h, and one can not locally eliminate σ_h and λ_h in favor of w_h.

Our time discretization follows Jameson's idea of dual time-stepping [12], which relies on classical backward difference (BDF) schemes. For an ordinary differential equation $y'(t) = f(y(t))$, these schemes can be written as

$$\sum_{i=0}^{l} \alpha_i y^{n+1-i} = \Delta t f(y^{n+1}).$$

for (constant) values α_i, $y^n \approx y(n\Delta t)$ and a given choice of Δt. BDF schemes are $A(\alpha)-$stable for $l \leq 6$ [9]. The first three BDF schemes are listed in Table 1. Obviously, all BDF schemes are implicit, however, similar to computing the steps in DIRK (diagonally implicit Runge-Kutta) methods, they are only implicit in y^{n+1}.

Name	l	α_0	α_1	α_2	$\alpha_3,$
implicit Euler	1	1	-1		
BDF2	2	$3/2$	-2	$1/2$	
BDF3	3	$11/6$	-3	$3/2$	$-1/3$

TABLE 1. BDF schemes

If we apply BDF to the scheme defined in (4), we obtain

$$\alpha_0 T(w_h^{n+1}, \varphi_h) + \Delta t N(\sigma_h^{n+1}, w_h^{n+1}, \lambda_h^{n+1}; \tau_h, \varphi_h, \mu_h) = -\sum_{i=1}^{l} \alpha_i T(w_h^{n+1-i}, \varphi_h),$$

which has to hold for all $(\tau_h, \varphi_h, \mu_h) \in H_h \times V_h \times M_h$.

For BDF schemes of order $l \geq 2$, it is necessary to have a 'startup' phase, i.e., one has to compute $(\sigma_h^k, w_h^k, \mu_h^k)$ for $k = 1, \ldots, l-1$ with a different method. We use the following strategy: For BDF2, it is enough to compute $(\sigma_h^1, w_h^1, \mu_h^1)$ by an implicit Euler step, as this method generates (in one step) approximations of $O(\Delta t^2)$. Unfortunately, for BDF3, such a simple strategy is not sufficient any more. To compute $(\sigma_h^1, w_h^1, \mu_h^1)$ and $(\sigma_h^2, w_h^2, \mu_h^2)$, we use a BDF2 scheme with time step $\widehat{\Delta t} := (\Delta t)^{\frac{3}{2}}$. This ensures that both quantities are approximations to the exact quantities of $O(\Delta t^3)$.

Obviously, the scheme in its current form has a lot of degrees of freedom. However, the unknowns associated to σ_h and w_h on a cell Ω_k are not directly coupled to the unknowns on another cell $\Omega_{k'}$, they are only implicitly coupled via λ. Thus, via local solution procedures (or, on the linear algebra level, via static condensation) [4], it is possible to express both σ_h and w_h as functions of λ_h only. Therefore, for each time step we obtain a nonlinear system of equations

$$M(\lambda_h, \mu_h) = b(\mu_h) \quad \forall \mu_h \in M_h,$$

which usually has less degrees of freedom than the corresponding DG discretization.

4. NUMERICAL RESULTS

4.1. **Linear convection-diffusion equation.** We consider a test case that has also been investigated by Nguyen et al. [14]. It is a scalar and linear convection-diffusion equation with the convective flux given as $f(w) = (-4y, 4x)^T w$, and the diffusive flux given as $f_v(w, \nabla w) = 0.1 \nabla w$. The source term g is set to 0, and the domain Ω is defined as $\Omega := [-0.5, 0.5]^2$. Note that in the vicinity of the origin, this problem is diffusion-dominated, as the convective flux vanishes. Away from $(0,0)$, convection gets more and more dominant. Based on the initial distribution, the exact solution can be chosen to be a rotating Gaussian distribution. We use a hybrid mixed method for this test case, i.e., we set $q = p + 1$. For $p = 0, 1, 2$, we perform a numerical convergence study. For $p = 0$, we use the implicit Euler scheme, for $p = 1$ we use a BDF2 scheme, and for $p = 2$, we use a BDF3 scheme. In all cases, the optimal order for w_h−convergence should be $p + 1$, which is observed, see Fig. 1 on the left. Note that for $p = 0$, the scheme needs much more time to get into the asymptotic regime. This is due to the rich spatial structure of the solution, which cannot be resolved well by a low-order scheme. In Fig. 1 on the right, we have plotted σ_h−convergence. For this test case, the order to be expected is $p + 1$ (which is also achieved), although σ_h is approximated in a space of polynomial order $p + 1$. This lack of optimality is due to the need for stabilization of the convective

terms, and is a common feature in mixed discretizations. For implications and ways to overcome this when diffusion is dominating, we refer to [7, 18].
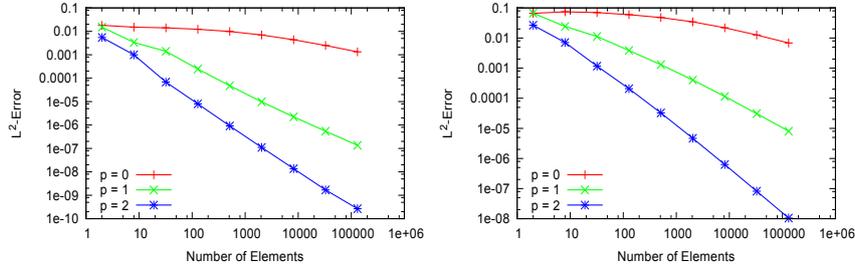

FIGURE 1. Convergence for the linear test case: w_h convergence (left) and σ_h convergence (right).

4.2. **Burgers equation.** The second test case under consideration is the multidimensional (viscous) Burgers equation with convective flux $f(w) = \frac{1}{2}(w^2, w^2)$ and viscous flux from Section 4.1, given as $f_v(w, \nabla w) = 0.1\nabla w$. The source term g is set in such a way that the exact solution for problem (1) can be given as

$$w(x, y, t) := e^{-t}\left(x + \frac{e^{10x} - 1}{1 - e^{10}}\right)\left(y + \frac{e^{10x} - 1}{1 - e^{10}}\right).$$

For this problem, we also use a hybrid mixed method, and perform for $p = 0, 1, 2$ a numerical convergence study. Again, temporal and spatial orders are chosen correspondingly. In all cases, convergence orders of $p + 1$ are achieved for both w_h and σ_h.
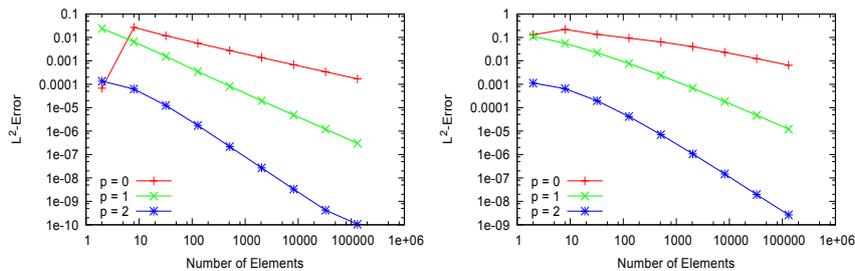

FIGURE 2. Convergence for Burgers equation: w_h convergence (left) and σ_h convergence (right).

4.3. **Navier-Stokes equations.** The flow past a circular cylinder is a classical example of a bluff body flow. When the Reynolds number is smaller than 50 the flow is steady and symmetric about the centerline of the wake. Even at small values of the Reynolds number, say Re = 10, the flow separates from the surface of the cylinder and forms a pair of bound vortices in the near wake. At Re = 50 this configuration becomes unstable and the process of vortex shedding begins, resulting in the well-known Karman vortex street.

We examine one configuration, defined by a Mach number Ma = 0.2 and a Reynolds number (based on the diameter of the cylinder) Re = 180. This test

case was also investigated in [8]. The employed mesh consists of 2916 elements and extends to 20 diameters away from the cylinder (a closer look at the wake region can be obtained in Fig. 3). At the cylinder wall no-slip conditions are applied; the outer boundary is modeled by characteristic far field conditions. We use the hybridized Discontinuous Galerkin method, i. e. $p = q$. The computations are initialized with free stream conditions.
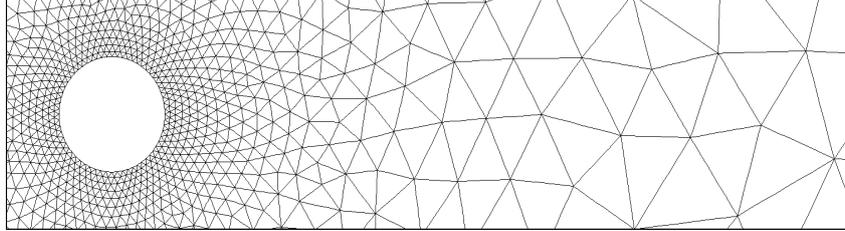

FIGURE 3. Close-up view of the employed mesh for the cylinder test case.

In Tables 2 and 3, the Strouhal numbers and the temporally averaged drag coefficients for various spatial and temporal discretizations are listed. Both numbers compare very well with shrinking time step to values from the literature (see Table 4). In Fig. 4, the Mach number is plotted at four temporal instances of the shedding cycle. The periodic nature of vortex shedding can be observed remarkably well (compare the first and the third, and the second and the fourth plot, respectively).

	BDF2			BDF3	
	$\Delta t = 1$	$\Delta t = 5$	$\Delta t = 10$	$\Delta t = 5$	$\Delta t = 10$
$p = 1$	0.1898	0.1585	0.1205	0.1931	0.1519
$p = 2$	0.1898	0.1618	0.1255	0.1964	0.1543
$p = 3$	0.1898	0.1618	0.1255	0.1964	0.1543

TABLE 2. Strouhal number for various spatial and temporal discretizations

|	BDF2			BDF3	
	$\Delta t = 1$	$\Delta t = 5$	$\Delta t = 10$	$\Delta t = 5$	$\Delta t = 10$
$p = 1$	1.3448	1.2449	1.0675	1.4604	1.4250
$p = 2$	1.3640	1.2486	1.0744	1.4972	1.4514
$p = 3$	1.3634	1.2490	1.0727	1.4795	1.4538

TABLE 3. Temporally averaged drag coefficient for various spatial and temporal discretizations

5. CONCLUSIONS AND OUTLOOK

We have presented a hybrid mixed method for the computation of time-dependent convection-diffusion equations, and we have demonstrated performance by numerical studies. One disadvantage of BDF methods is that they do not allow for (arbitrary) high order discretizations, as they become unstable for $l \geq 7$. One very

Experiment	c_D	Sr
Gopinath [8]	1.3406	0.1866
Henderson [11]	1.336	-
Williamson [20]	-	0.1919

TABLE 4. Mean drag coefficients and Strouhal numbers from the literature
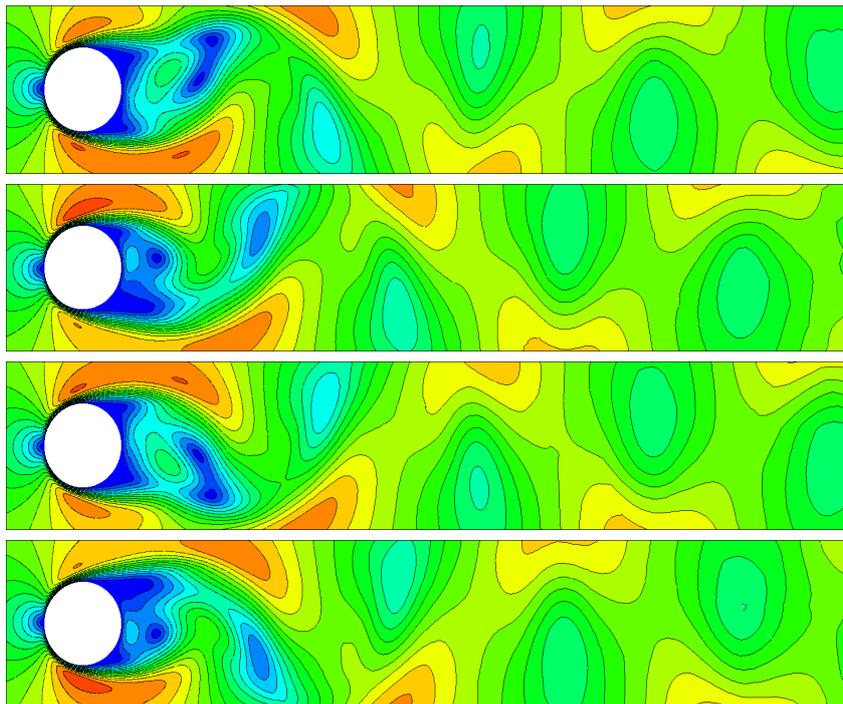
FIGURE 4. Four subsequent snapshots of the vortex shedding cycle ($p = 3$, BDF2, $\Delta t = 1$).

near-future project is the incorporation of time-spectral methods to simulate periodic flows, such as the flow past the circular cylinder, more efficiently. This would also allow to compute more involved test cases, such as (periodically) flapping wings.

Furthermore, stability of our method has not yet been investigated theoretically. For the limiting cases of the underlying equation (1), i.e., $f \equiv 0$ or $f_v \equiv 0$, it is well-known that the semi-discretization in (4) is L^2-stable. However, this has yet to be shown for the full convection-diffusion equation. Also for the fully discretized scheme, stability has still to be shown.

REFERENCES

[1] F. Bassi and S. Rebay *A High-Order Accurate Discontinuous Finite-Element Method for the Numerical Solution of the Compressible Navier-Stokes Equations* Journal of Computational Physics, 1997, 131, 267–279

[2] F. Brezzi, J. Douglas and L. D. Marini *Two Families of Mixed Finite Elements for Second Order Elliptic Problems* Numerische Mathematik, 1985, 47, 217–235

[3] F. Brezzi and M. Fortin *Mixed and Hybrid Finite Element Methods* Springer Series in Computational Mathematics, New York, 1991

[4] B. Cockburn and J. Gopalakrishnan *A Characterization of Hybridized Mixed Methods for Second Order Elliptic Problems* SIAM J. Numer. Anal., 2004, 42, 283–301

[5] B. Cockburn, J. Gopalakrishnan and R. Lazarov *Unified Hybridization of Discontinuous Galerkin, Mixed, and Continuous Galerkin Methods for Second Order Elliptic Problems* SIAM J. Numer. Anal., 2009, 47, 1319–1365

[6] B. Cockburn and C.-W. Shu *TVB Runge-Kutta Local Projection Discontinuous Galerkin Finite Element Method for Conservation Laws II: General Framework* Mathematics of Computation, 1988, 52, 411–435

[7] H. Egger and J. Schöberl *A Hybrid Mixed Discontinuous Galerkin Finite Element Method for Convection-Diffusion Problems* IMA Journal of Numerical Analysis, 2010, 30, 1206–1234

[8] A. Gopinath and A. Jameson *Application of the time spectral method to periodic unsteady vortex shedding* AIAA Paper 2006-0449, 2006

[9] E. Hairer and G. Wanner *Solving Ordinary Differential Equations II* Springer Series in Computational Mathematics, Berlin Heidelberg, 1991

[10] R. Hartmann *Adaptive Discontinuous Galerkin methods with shock-capturing for the compressible Navier-Stokes equations* International Journal for Numerical Methods in fluids, 2006, 51, 1131–1156

[11] R.D. Henderson *Details of the drag curve near the onset of vortex shedding* Physics of Fluids, 1995, 7

[12] A. Jameson *Time dependent calculations using multigrid, with applications to unsteady flows past airfoils and wings* AIAA Paper 1991-1596, 1991

[13] D. Ketcheson, C. Macdonald and S. Gottlieb *Optimal implicit strong stability preserving Runge-Kutta methods* Appl. Numer. Math., 2009, 59, 373-392

[14] N. Nguyen, J. Peraire and B. Cockburn *An implicit high-order hybridizable Discontinuous Galerkin method for linear convection-diffusion equations* Journal of Computational Physics, 2009, 228, 3232–3254

[15] N. Nguyen, J. Peraire and B. Cockburn *An implicit high-order hybridizable Discontinuous Galerkin method for nonlinear convection-diffusion equations* Journal of Computational Physics, 2009, 228, 8841–8855

[16] J. Peraire, N. Nguyen and B. Cockburn *A Hybridizable Discontinuous Galerkin Method for the Compressible Euler and Navier-Stokes Equations* AIAA Paper 2010-363, 2010

[17] J. Schütz and G. May *A Hybrid Mixed Method for the Compressible Navier-Stokes Equations* Submitted to the Journal of Computational Physics, 2011

[18] J. Schütz, M. Woopen and G. May *A Hybridized DG/Mixed Scheme for Nonlinear Advection-Diffusion Systems, Including the Compressible Navier-Stokes Equations* AIAA Paper 2012-0729, 2012

[19] J. Schütz and G. May *An Adjoint Consistency Analysis for a Class of Hybrid Mixed methods* IGPM preprint Nr. 336, 2012

[20] C.H.K. Williamson *Vortex dynamics in the cylinder wake* Annual review of fluid mechanics, 1996, 28, 477–539

E-mail address: `schuetz@igpm.rwth-aachen.de`
E-mail address: `woopen@aices.rwth-aachen.de`
E-mail address: `may@aices.rwth-aachen.de`